Thermal Mechanical Coupling Analysis of a Flexible Spoke Non-pneumatic Tire

Hongxun Fu – Xuemeng Liang – Yan Wang – Laiyun Ku – Zhen Xiao

Shandong University of Technology, School of Transportation and Vehicle Engineering, China

A new type of non-pneumatic tire with a flexible spoke structure is proposed to solve traditional pneumatic tire defects, such as easy bursting, the requirement of real-time maintenance to keep tire pressure, and a complex manufacturing process. The thermal mechanical coupling characteristics of the flexible spoke non-pneumatic tire are studied in detail to obtain the steady-state temperature field distribution pattern under different operating conditions. A unit configuration method is proposed to build the 3D model of the flexible spoke non-pneumatic tire. Then, the thermal-mechanical sequential coupling method is used to analyse the deformation, energy loss and heat conduction of the flexible spoke non-pneumatic tire. Finally, the steady-state temperature field distribution pattern under thermal-mechanical coupling is obtained. The results show that the high temperature region of the non-pneumatic tire is mainly distributed in the middle bending part of the flexible spoke unit, and the temperature gradually decreases from the centre of the flexible spoke to the surrounding parts. The influence of load on the temperature change of non-pneumatic tire is greater than that of the driving speed. This study provides a theoretical basis and method guidance for solving the failure problem of the non-pneumatic tires under the action of thermal-mechanical coupling.

Keywords: non-pneumatic tire, flexible spoke structure, unit configuration method, thermal mechanical coupling, temperature field

Highlights
- A unit configuration method for the structural design of the non-pneumatic tire is proposed.
- The thermal-mechanical sequential coupling method is used to analyse the deformation, energy loss, and heat conduction of the flexible spoke non-pneumatic tire.
- The temperature field distribution pattern of the flexible spoke non-pneumatic tire under the influence of thermal mechanical coupling is obtained.
- The influence of load on the temperature change of the non-pneumatic tire is greater than that of driving speed.

0 INTRODUCTION

A non-pneumatic tire does not rely on air to adjust the tire elasticity and support the weight of the vehicle. It solves the problems of the traditional pneumatic tire, such as easy bursting, the requirement of real-time maintenance to keep tire pressure, and a complex manufacturing process. Therefore, non-pneumatic tire technology has gradually become a research topic of great interest in the field of tire safety, and new types of non-pneumatic tire structures have been put forward [1] to [3]. Compared with pneumatic tires, non-pneumatic tires have the advantages of anti-puncture, explosion-proof, shock absorption and good adhesion performance. However, they have poor performance in reliability and durability as they are easily affected by stress concentrations, alternating stresses, high temperatures and other factors [4] and [5]. The above problems seriously restrict the further development and application of non-pneumatic tire technology. Based on the study of the basic mechanical properties of a non-pneumatic tire, thermal analysis of a non-pneumatic tire has also been conducted. Currently, the performance of a non-pneumatic tire under the action of thermo-mechanical couplings has been

analysed. This has a high theoretical significance and an application value for the development of tire safety technology [6] to [8].

Researchers have conducted studies on the basic mechanical properties, fatigue, failure of non-pneumatic tires. Gasmi et al. [9] and Kucewicz et al. [10] conducted vertical static deflection simulations with the Tweel™ and honeycomb tires, analysing the influence of the vertical displacement of the hub, tread deformation and grounding pressure on the geometry of the flexible spoke structure. Xu et al. [11] studied the influence of the ratio of the mechanical elastic wheel (MEW) hinge group length to the elastic wheel thickness on the radial stiffness of the wheel based on the finite element analysis, realizing the multi-objective optimization of the radial stiffness of the MEW based on the artificial fish swarm algorithm. Mazur et al. [12], Ju et al. [13] and Jackowski et al. [14] obtained the rolling resistance of a non-pneumatic tire based on the prototype test method; they studied the influence of tire structure and the polyurethane (PU) material on the rolling resistance of a non-pneumatic tire, and compared pneumatic and non-pneumatic tires in terms of the rolling resistance. Fu et al. [15] and [16] conducted a preliminary study on the lateral deflection

143

properties of a mechanical elastic wheel and its influencing factors and established a theoretical model of the lateral loading of the wheel. Zang et al. [17] and Du et al. [18] studied the influences of load and roll angle on the distribution of the contact pressure of a MEW and made a comparison with the pneumatic tire. Sriwijaya and Hamzah [19] studied the influence of the road inclination angle on the stress distribution of the flexible spoke structure of a non-pneumatic tire; their results show that a larger road inclination angle increases the equivalent stress value of a honeycomb flexible spoke structure, thus accelerating the failure of the flexible spoke structure. Zhang et al. [20] carried out a static grounding performance analysis of a staggered non-pneumatic tire, obtaining the S-N curve of the flexible spoke PU material by using the demosia fatigue test, and entering it into the FE-SAFE software to predict the tire fatigue life. The above studies have preliminarily explored the structural performance and fatigue failure of a non-pneumatic tire, but the influence of temperature has not been considered in the research process.

During the rolling motion, the non-pneumatic tire deforms under the action of external loads, which causes a temperature rise of the tire, resulting in a possible decline of physical and chemical properties of the tire materials, a loss of strength, and eventually tire failure [21] and [22]. Many studies have been carried out to evaluate both the performance and the durability of pneumatic tires with temperature, but there are few studies on the influence of temperature of non-pneumatic tires. In particular, Chen et al. [23] and Zhu et al. [24] analysed the effects of vehicle speed, loss factor, and thermal conductivity of the material and wheel section width on the maximum temperature of a MEW. The authors proposed a theoretical analysis method to predict the surface temperature of a MEW under different driving conditions.

In this paper, the three dimensional (3D) model and numerical analysis model of a 195/50N16 flexible spoke non-pneumatic tire were established based on the unit configuration method. The thermo-mechanical sequential coupling method was used to investigate the thermo-mechanical coupling characteristics of the flexible spoke non-pneumatic tire under different operating conditions, which provides a method guidance for the subsequent fatigue failure research and structural optimization design of non-pneumatic tires.

1 ESTABLISHMENT OF THE NUMERICAL ANALYSIS MODEL OF A FLEXIBLE SPOKE NON-PNEUMATIC TIRE

1.1 Establishment of the 3D Model of the Flexible Spoke Non-pneumatic Tire using the Unit Configuration Method

Our research group proposed a unit configuration method for modelling the structural design of the non-pneumatic tire. It creates the non-pneumatic tire model of different structures by combining the unit structure with an arbitrary shape according to a different array mode and array number.

In this paper, the flexible spoke support body of the flexible spoke non-pneumatic tire consists of a circular array of 45 groups of flexible spoke units. Every group occupies a construction angle of 8°. Each flexible spoke unit consists of an inner ring, a circumferential spoke, a side spoke, and an outer
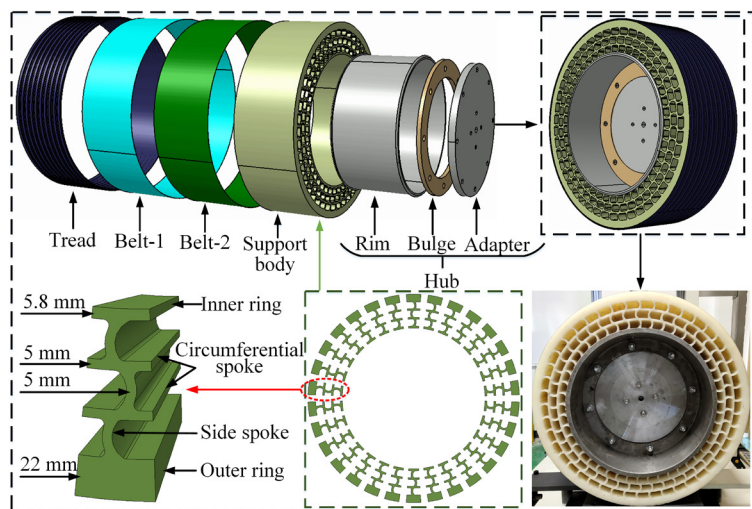
Fig. 1. *3D model of the flexible spoke non-pneumatic tire*

ring. The circumferential spokes of the flexible spokes are arranged in a layered structure along the radial direction of the tire, and the side spokes of the flexible spokes are combined as a wave line by "curved surface" treatment, with a curvature of 1/15. The flexible spoke non-pneumatic tire comprises a rigid hub, a flexible spoke support body made of PU material and a rubber tread. The flexible spoke support body connects the hub and the tread as a whole. In this case, the rigid hub is composed of the rim, the hub bulge and the hub adapter assembly, and the rubber tread contains two layers of wire belt. The flexible spoke non-pneumatic tire based on the unit configuration method is shown in Fig. 1, and the detailed structural parameters are shown in Table 1.

Table 1. *Detailed structural parameters of the tire*

Structure	Parameters
Tire model	195/50N16
Tread width [mm]	195
Outside diameter [mm]	602
Rim diameter [mm]	406.4
Spoke thickness [mm]	5
Curvature of spoke	1/15
Construction angle [°]	8
Number of unit groups	45

1.2 Construction of Numerical Analysis Model

The flexible spoke support body is the main structure of the flexible spoke non-pneumatic tire. The heat generation of the entire tire mainly comes from the flexible spoke support body. In the steady-state rolling process, the frictional heat generated by the contact between the tread and the ground is small and quickly carried away by the air, which has little influence on the overall temperature distribution of the flexible spoke non-pneumatic tire.

Therefore, the influence of the tread on the temperature distribution of the flexible spoke non-pneumatic tire can be ignored in the numerical analysis. To obtain the basic material properties of the PU material forming the flexible spoke support body, uniaxial tensile tests of the PU material were carried out by using an electronic universal testing machine to obtain the stress-strain relationship, as shown in Fig. 2.

For nonlinear materials, both the fitting accuracy and the stability are high by using Yeoh material constitutive model. The strain energy function of the hyper-elastic Yeoh model is as follows:

$$W = \sum_{i=1}^{3} C_{i0}(\overline{I}_1 - 3)^i$$
$$= C_{10}(\overline{I}_1 - 3) + C_{20}(\overline{I}_1 - 3)^2 + C_{30}(\overline{I}_1 - 3)^3, \quad (1)$$

where W is strain energy density; $\overline{I}_1$ is the first invariant of principal elongation ratio; C_{10}, C_{20}, C_{30} are material constants. In the first step of our study, the PU material is modelled as nonlinear elastic for simplification. Based on this approach, the mechanical loadings in the spokes of the non-pneumatic tire can be estimated.
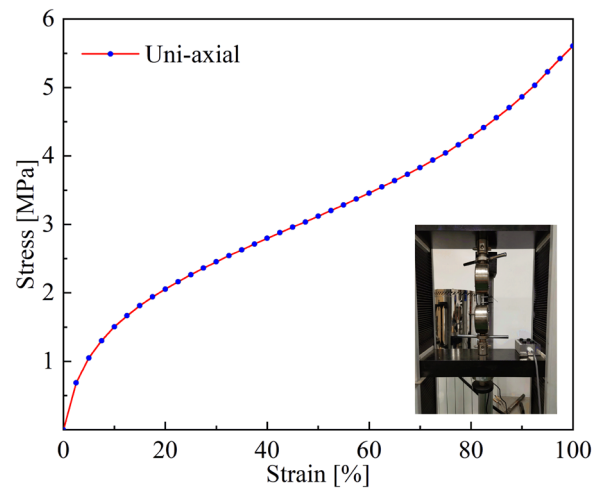
Fig. 2. *Stress-strain relationship of PU material*

The mesh of the flexible spoke non-pneumatic tire was divided. Since the hexahedral element has a higher accuracy in the calculations and is convenient for extracting the stress and the strain of the flexible spoke unit, the mesh of the flexible spoke unit consists of C3D8RH elements. The element number of a flexible spoke unit was 6,909, and that of the entire flexible spoke non-pneumatic tire was 193,050. The analysis steps and interaction settings of the flexible spoke non-pneumatic tire were carried out, and the friction coefficient was set to 0.5.

1.3 Verification of the Effectiveness of the Numerical Analysis Model

The static analysis of the flexible spoke non-pneumatic tire was carried out in ABAQUS, and the vertical load was evenly increased to the maximum level of 5000 N with intervals of 500 N. The loading test of the flexible spoke non-pneumatic tire under the same working condition was carried out based on the tire testing machine. After the completion of the test, the axial sinking under different vertical loads was

extracted, and the simulated and measured data were presented as vertical stiffness curves. The comparison of vertical stiffness curves of the flexible spoke non-pneumatic tire simulation and the test is shown in Fig. 3. RP represents the centre of the flexible spoke non-pneumatic tire.

It can be seen from Fig. 3 that the vertical stiffness of the flexible spoke non-pneumatic tire in the simulation and test tended to be consistent. After calculation, the relative error between the simulation and the test verification was only 4.7 %, which demonstrates the accuracy of the numerical analysis model.
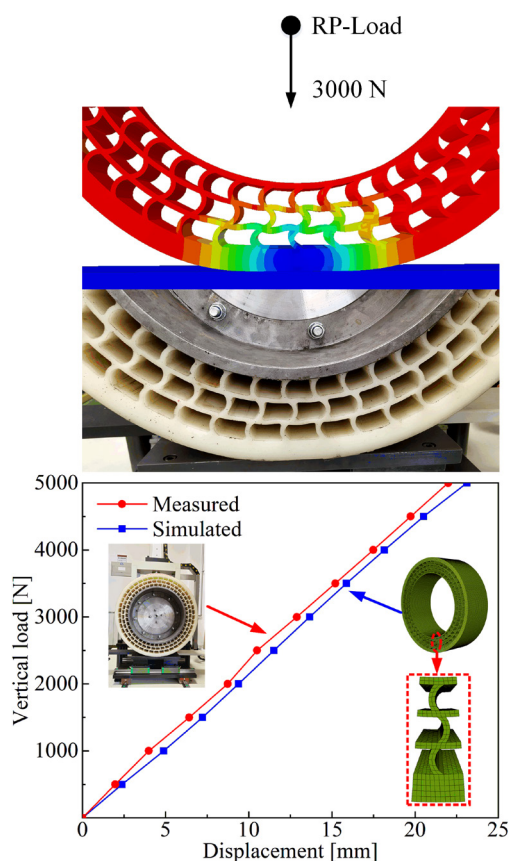
Fig. 3. *Comparison of vertical stiffness curves of simulation and test*

2 THERMAL-MECHANICAL COUPLING ANALYSIS OF THE FLEXIBLE SPOKE NON-PNEUMATIC TIRE

2.1 Thermal-mechanical Sequential Coupling Method

In this study, the thermo-mechanical sequential coupling method was used to analyse the mechanical fields of the flexible spoke non-pneumatic tire firstly,

and then the analysis results of mechanical fields were used as input conditions for the thermal field analysis. Finally, the thermo-mechanical coupling characteristics of the flexible spoke non-pneumatic tire were obtained. Fig. 4 shows the flow chart of the thermo-mechanical coupling analysis of the flexible spoke non-pneumatic tire, which mainly consists of deformation analysis, energy loss analysis and heat conduction analysis. In the deformation analysis, the static and dynamic mechanical characteristics were analysed using ABAQUS software. The accuracy of the numerical analysis model was verified in the static analysis. The stress and strain of each mesh element during the steady-state rolling process of a flexible spoke unit were extracted in the dynamic analysis. In the energy loss analysis, a Fourier transformation of the equivalent stress and equivalent strain was carried out using MATLAB software, and the lagging energy loss and heat generation rate were calculated. In the heat conduction analysis, a user subroutine was written to define the internal heat source, to endow the material with thermal properties and to set the thermal boundary conditions. Finally, the steady-state temperature field distribution pattern of the flexible spoke non-pneumatic tire under thermal-mechanical coupling was obtained.

2.2 Deformation Analysis

In the deformation analysis, the steady-state rolling of the flexible spoke non-pneumatic tire was carried out under a vertical load of 5000 N and driving speeds of 45 km/h, 65 km/h and 85 km/h, respectively. When the driving speed was 85 km/h, vertical loads of 3000 N, 4000 N, and 5000 N were applied to the non-pneumatic tire. The stress and strain of each mesh element in the flexible spoke unit under a rolling period (one cycle) were extracted. The data contained a total of 90 stress and strain data sets in one rolling period. Each set contains six components: S11 (LE11), S22 (LE22), S33 (LE33), S12 (LE12), S13 (LE13) and S23 (LE23). It was extracted once per mesh element at an interval of 4°. The stress and strain curves of a mesh element under a load of 5000 N and a driving speed of 85 km/h are shown in Fig. 5. This work provides a source of data for subsequent calculations of equivalent stress and equivalent strain.

2.3 Energy Loss Analysis

Fig. 6 shows the stress-strain phase diagram of the viscoelastic PU material. It can be seen that the stress and the strain of PU are not synchronized during
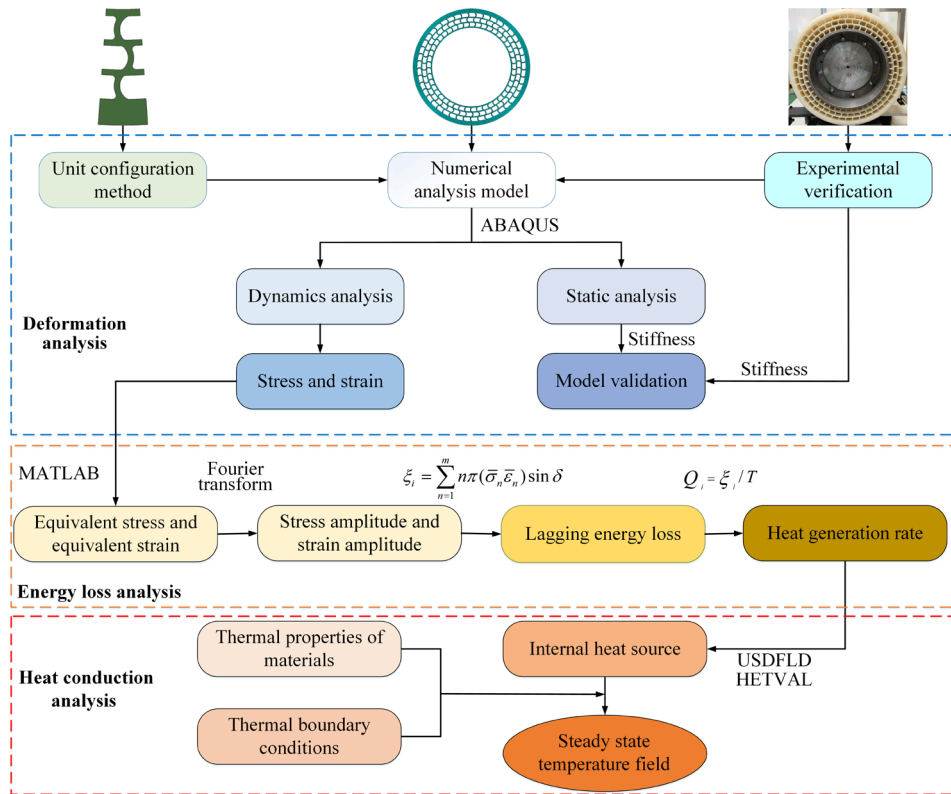
Fig. 4. *Flow chart of thermal mechanical coupling characteristics analysis*
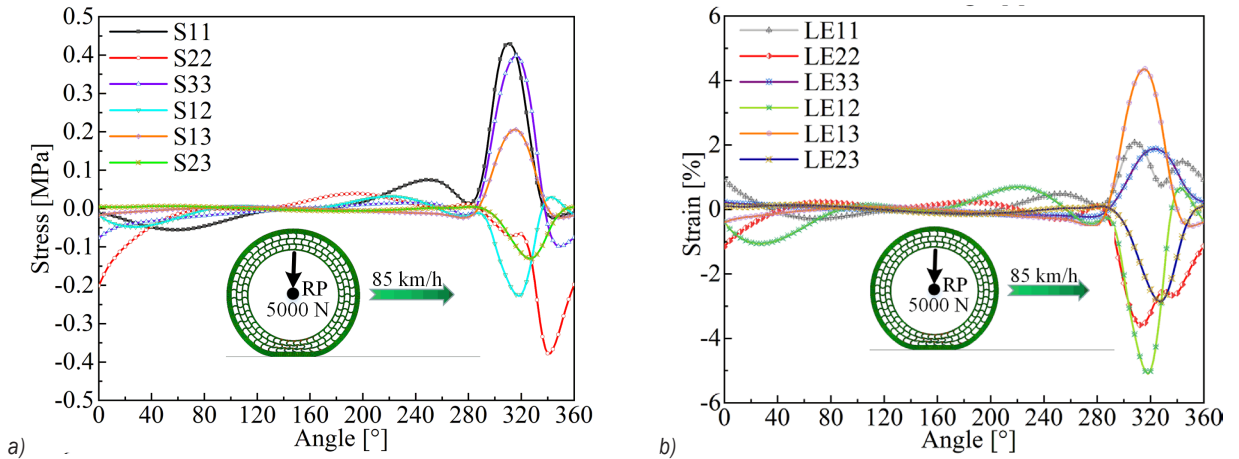
Fig. 5. *a) Stress and b) strain curve of a mesh element*

deformation, and the lagging phase angle δ appeared, as shown in Fig. 6a. Under the action of a cyclic load, the non-synchronization of stress and strain caused a hysteresis loop in the stress-strain curve of the material. The hysteresis area is basically the energy loss of the viscoelastic material, as shown in Fig. 6b. Assuming that the PU material is subjected to sinusoidal stress and strain, both variables can be expressed as:

$$\begin{cases} \sigma = \sigma_0 \sin(\omega t + \delta), \\ \varepsilon = \varepsilon_0 \sin\omega t \end{cases} \qquad (2)$$

where σ is the stress; ε is the strain; σ_0 is the stress amplitude; ε_0 is the strain amplitude; ω is the angular frequency; δ is the lagging phase angle; t is the time.

According to the stress-strain relationship, the energy loss of the non-pneumatic tire in a rolling period T can be expressed as:

$$\xi = \int_0^T \sigma d\varepsilon. \qquad (3)$$

Substituting Eq. (2) into Eq. (3) yields:

$$\xi = \pi\sigma_0\varepsilon_0\sin\delta, \qquad (4)$$

where, $\sin \delta$ is the energy loss coefficient.

a)

b)
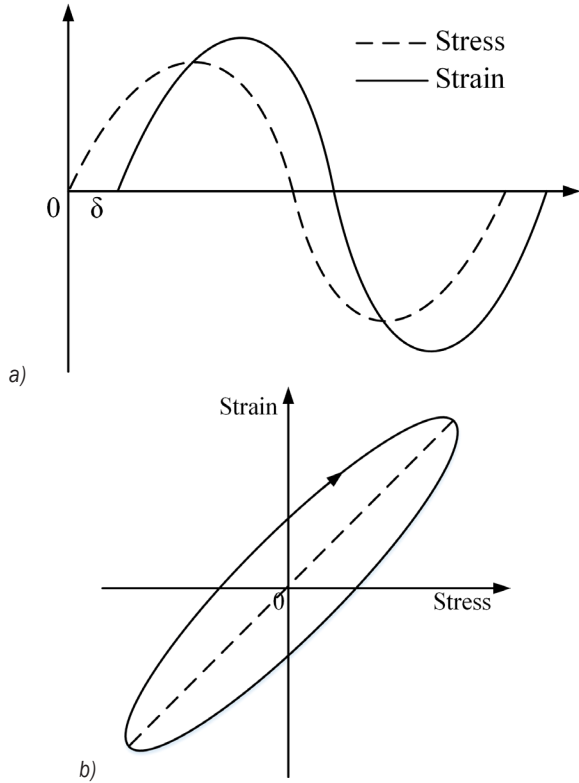
Fig. 6. *Stress-strain phase diagram;*
a) stress-strain phase relationship, and b) lagging loop

The energy loss of nonlinear viscoelastic PU materials mainly comes from the deformation of the materials. According to the strength theory of materials, the state of nonlinear materials can be expressed by an equivalent stress and an equivalent strain, which can be expressed as follows:

$$\begin{cases} \bar{\sigma} = \dfrac{3}{2\sqrt{2}}[(\sigma_x - \sigma_y)^2 + (\sigma_y - \sigma_z)^2 \\ + (\sigma_z - \sigma_x)^2 + 6(\sigma_{xy}^2 + \sigma_{yz}^2 + \sigma_{zx}^2)]^{1/2} \\ \bar{\varepsilon} = \dfrac{3}{2\sqrt{2}}[(\varepsilon_x - \varepsilon_y)^2 + (\varepsilon_y - \varepsilon_z)^2 \\ + (\varepsilon_z - \varepsilon_x)^2 + 6(\varepsilon_{xy}^2 + \varepsilon_{yz}^2 + \varepsilon_{zx}^2)]^{1/2} \end{cases} \qquad (5)$$

According to Eq. (5), the equivalent stress $\bar{\sigma}$ and the equivalent strain $\bar{\varepsilon}$ of each mesh element were calculated in MATLAB, and fitted by the Fourier

series fitting method based on the least square method. The related equation is as follows:

$$\begin{cases} \sigma = \sigma_0 + \sum_{n=1}^{m}[\sigma_{1n}\cos(n\omega t) + \sigma_{2n}\sin(n\omega t)] \\ = \sigma_0 + \sum_{n=1}^{m}\sqrt{\sigma_{1n}^2 + \sigma_{2n}^2}\,\sin(n\omega t + \theta_{\sigma n}) \\ \varepsilon = \varepsilon_0 + \sum_{n=1}^{m}[\varepsilon_{1n}\cos(n\omega t) + \varepsilon_{2n}\sin(n\omega t)] \\ = \varepsilon_0 + \sum_{n=1}^{m}\sqrt{\varepsilon_{1n}^2 + \varepsilon_{2n}^2}\,\sin(n\omega t + \theta_{\varepsilon n}) \end{cases} \qquad (6)$$

The constant m represents the fitting order. For most of the data, when $m = 8$, a better fitting value can be obtained, but a small part of the data loses its meaning. Therefore, we set five different orders of fitting from $m = 8$ to $m = 4$; when $m = 8$, the data lose its meaning, $m = 7$ will be used for fitting, and so on.

a)

b)
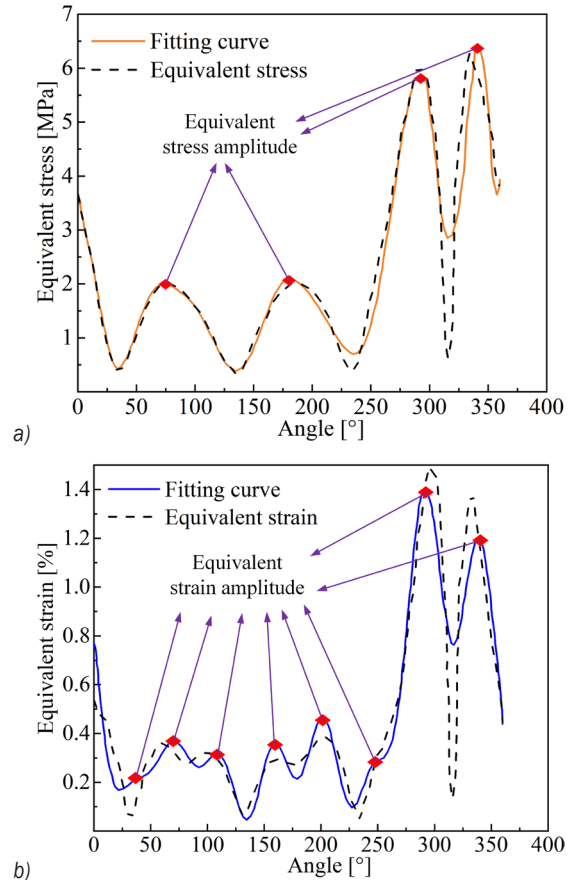
Fig. 7. *Fitting curve of equivalent stress and strain of a mesh element; a) equivalent stress; b) equivalent strain*

Fig. 7 shows the fitting curves of the equivalent stress and the equivalent strain of a randomly selected mesh element. It is clear that the equivalent stress and

equivalent strain cycle are anharmonic under steady-state rolling conditions. For the equivalent stress and equivalent strain cycle of anharmonic variation, it is necessary to express them as the superposition of a group of harmonics by the Fourier transformation, so as to obtain the equivalent stress amplitude and equivalent strain amplitude of each harmonic component at its corresponding frequency.

According to Eq. (6), the corresponding equivalent stress amplitude $\bar{\sigma}_n$ and equivalent strain amplitude $\bar{\varepsilon}_n$ can be calculated as follows:

$$\begin{cases} \bar{\sigma}_n = \sqrt{\sigma_{1n}{}^2 + \sigma_{2n}{}^2} \\ \bar{\varepsilon}_n = \sqrt{\varepsilon_{1n}{}^2 + \varepsilon_{2n}{}^2} \end{cases}. \qquad (7)$$

According to Eqs. (4) and (7), the energy loss ξ_i of each mesh element of the flexible spoke non-pneumatic tire in one rolling period T can be calculated according to Eq. (8):

$$\xi_i = \sum_{n=1}^{m} n\pi(\bar{\sigma}_n\bar{\varepsilon}_n)\sin\delta. \qquad (8)$$

The constant $\bar{\sigma}_n$ represents the equivalent stress amplitude; $\bar{\varepsilon}_n$ represents the equivalent strain amplitude; $\sin\delta$ represents the energy loss coefficient; m is the fitting order; i represents the element number (1 to 4170).

The ratio of the energy loss of each mesh element to the rolling period T is equal to the heat generation rate Q_i of each element, which can be expressed as follows:

$$Q_i = \xi_i / T, \qquad (9)$$

here, ξ_i is the energy loss of each mesh element, T is the rolling period, $T = \pi d / v$ in [s], d is the outer diameter of the tire [m], and v is the tire rolling speed [m/s].

2.4 Heat Conduction Analysis

In the heat conduction analysis, the heat generation rate calculated by ABAQUS is assigned to each mesh element as the heat load to complete the definition of the internal heat source. In this paper, two subroutines were used to define the internal heat sources: the subroutines USDFLD was used to redefine the field variables, and the subroutine HETVAL was used to define the internal heat source.

For the numerical simulation of the temperature field of the non-pneumatic tire, the following four assumptions are generally considered:

(1) The material properties of each part of the non-pneumatic tire are not influenced by temperature, and the entire energy loss in the rolling process is converted into heat, without heat loss.
(2) The temperature distribution is steady, and there is no temperature gradient in the circumferential direction of the non-pneumatic tire, meaning that the temperature distribution of each flexible spoke unit is exactly the same.
(3) The material of each part of the tire is isotropic.
(4) The non-pneumatic tire will be in thermal equilibrium after rolling at a constant speed for some time.

According to the above assumptions, the material is endowed with thermal properties and thermal boundary conditions are set. The thermal properties of the PU material mainly include thermal conductivity, thermal expansion coefficient, specific heat and convective thermal transfer coefficient, as shown in Table 2.

Table 2. *Thermal properties of PU material*

Thermal properties	Parameter
Thermal conductivity k [W/(m·K)]	0.3
Thermal expansion coefficient a [°C⁻¹]	0.0002
Specific heat c [J/(kg·K)]	2×10^9

The thermal boundary conditions of the flexible spoke non-pneumatic tire include the tread boundary in contact with the ground, body surface boundary in contact with air and inner circle boundary in contact with the rigid hub. In the actual rolling process, the heat exchange between the tread and the road, as well as that between the flexible spoke inner ring and the rigid hub, can be calculated in the form of thermal conduction. The heat exchange between the flexible spoke support body and the air can be calculated in the form of convective thermal transfer. The convective heat transfer coefficient is approximately described according to the following equation:

$$h = 2.2v^{0.84}, \qquad (10)$$

here, h is the convective heat transfer coefficient of the surface boundary of the body [W/(m²·K)], and v is the tire rolling speed in [m/s].

3 RESULT ANALYSIS

3.1 Analysis of Overall Distribution Trend of Steady-state Temperature Field

Fig. 8 shows the comparison diagram of steady-state temperature field distribution and the stress distribution under a vertical load of 5000 N and a driving speed of 85 km/h. The vertical load led to greater deformation in the middle part of the flexible spoke unit, causing greater stress and strain and increased energy loss, resulting in more heat generation. Therefore, the high-temperature region is mainly distributed in the middle bending part of the flexible spoke unit, which is consistent with the main stress deformation part. The overall temperature gradually decreases from the centre of the flexible spoke unit to the surrounding area, and the central temperature reached 71.9 °C. The problem of local high temperatures can be solved by improving the structure of the flexible spoke unit and reducing the stress concentration.

3.2 Influence of Driving Speed on Steady-state Temperature Field Distribution

Fig. 9 shows the steady-state temperature field distribution trend of the flexible spoke non-pneumatic tire under a vertical load of 5000 N at different driving speeds. Figs. 9a, b, and c show the temperature distributions of a flexible spoke unit for different driving speeds; Figs. 9d and e show the temperature distribution trend maps of each node on the vertical axis and lateral axis of flexible spoke unit. According to Figs. 9a, b, and c, with the increase in the driving speed, the temperature distribution of the flexible spoke non-pneumatic tire was almost unchanged. This indicates that the driving speed did not influence the temperature distribution patterns and characteristics of the non-pneumatic tire, but both the overall temperature and the maximum temperature slightly increase with the increase of the driving speed; in fact, the maximum temperature increased from 58.3 °C to 71.9 °C. According to the energy loss analysis, with the increase of driving speed, the rolling period of the non-pneumatic tire became gradually shorter. The heat generation rate of each mesh element increased as well, which implies the overall temperature of the non-pneumatic tire increased. It can be seen from Figs. 9d and e that under different driving speeds, the node temperature on the vertical axis and lateral axis of the flexible spoke unit showed a tendency of first increasing and then decreasing, and the temperature at the centre of the flexible spoke was higher than that at the edge of it. With the increase of driving speed, the temperature rise in the centre of the flexible spoke is greater than that at the edge of it. When the driving speed increased from 45 km/h to 65 km/h, the maximum temperature of the node was increased by 4.19 °C; when the driving speed increased from 65 km/h to 85 km/h, the maximum temperature of the node was increased by 8.44 °C, indicating that the influence of the driving speed on the temperature change of the non-pneumatic tire is greater under high speed than under the low speed condition.
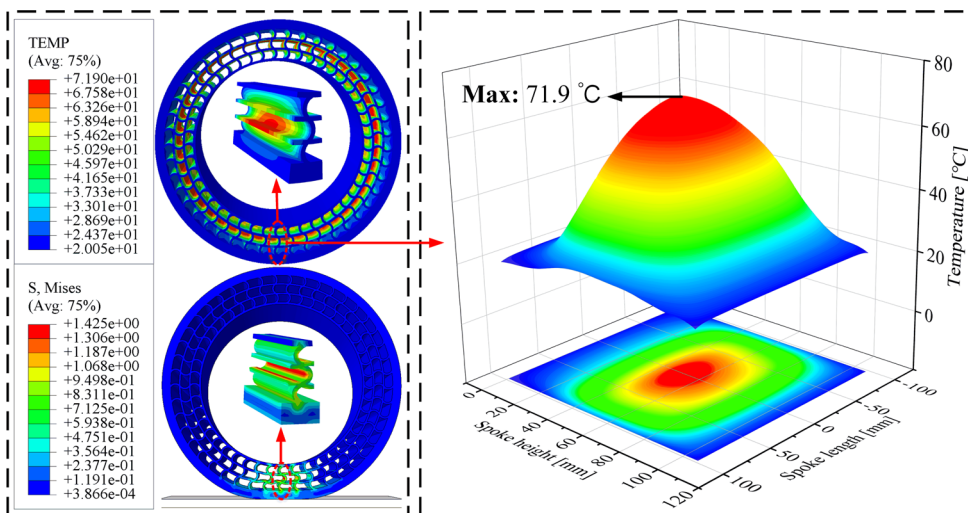
Fig. 8. *Comparison diagram of steady-state temperature field distribution and stress distribution*
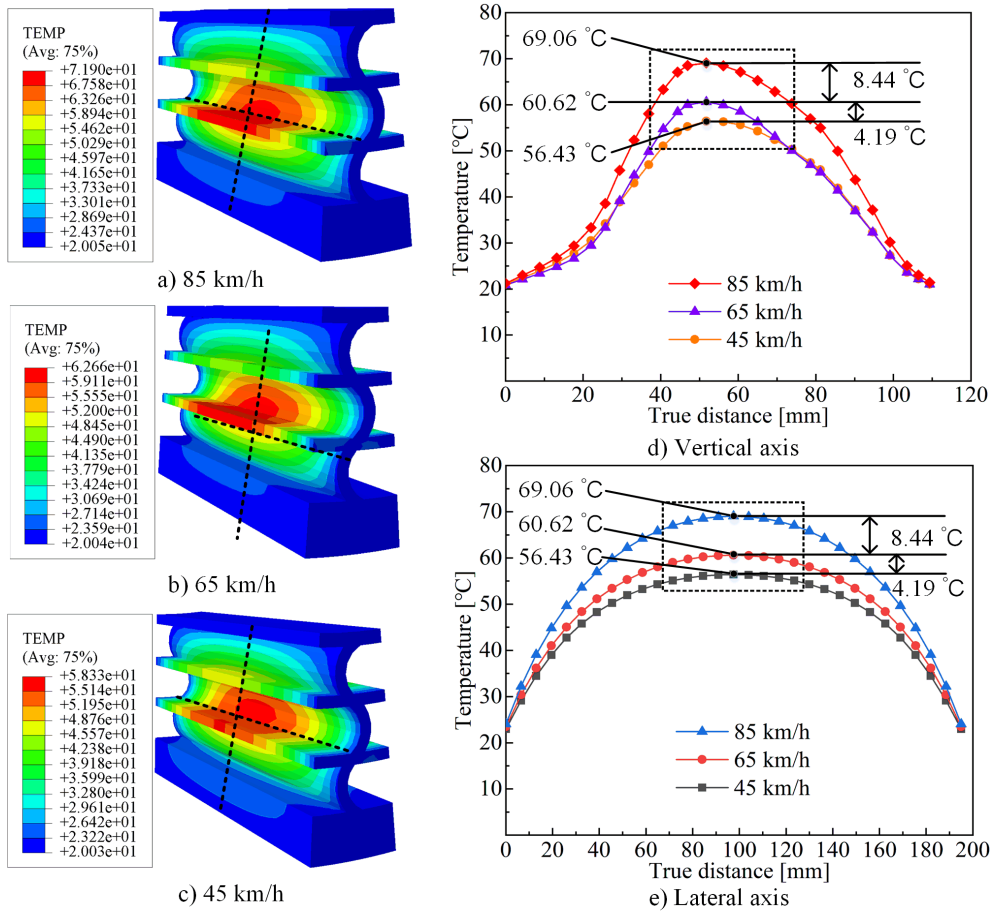
Fig. 9. *Steady-state temperature field distribution under different driving speeds*

3.3 Influence of Load on Steady-state Temperature Field Distribution

Fig. 10 shows the steady-state temperature field distribution trend of the flexible spoke non-pneumatic tire under different loads at the driving speed of 85 km/h. Figs. 10a, b, and c show the temperature field distribution maps of the flexible spoke unit under different loads, and Figs. 10d and e show the temperature distribution trend maps of each node on the vertical axis and lateral axis of the flexible spoke unit.

According to Figs. 10 a, b, and c, the change of load has little influence on the temperature distribution of the flexible spoke non-pneumatic tire, and the high-temperature region always existed in the central part of the flexible spoke unit. However, the overall and maximum temperature of the non-pneumatic tire increased significantly with the increase of the load, and, in fact, the maximum temperature increases

from 31.9 °C to 71.9 °C. According to the energy loss analysis, with the increase of the load, the sinking amount of non-pneumatic tire gradually increased, and the deformation amplitude of each part of the tire increased as well, which increased the stress amplitude, strain amplitude, and the energy loss of each mesh element, resulting in an increase of the heat generation rate. It can be seen from Figs. 10 d and e that under different loads, the node temperature on the vertical axis and lateral axis of the flexible spoke unit showed a tendency of first increasing and then decreasing, and the temperature at the centre of the flexible spoke was higher than that at the edge of the flexible spoke. With the increase of the load, the temperature rise at the centre of the flexible spoke was significantly greater than that at the edge of the flexible spoke. In addition, the temperature rise amplitude caused by the load increasing from 3000 N to 4000 N was almost the same as that caused by the load increasing from 4000 N to 5000 N. This

Thermal Mechanical Coupling Analysis of a Flexible Spoke Non-pneumatic Tire   **151**
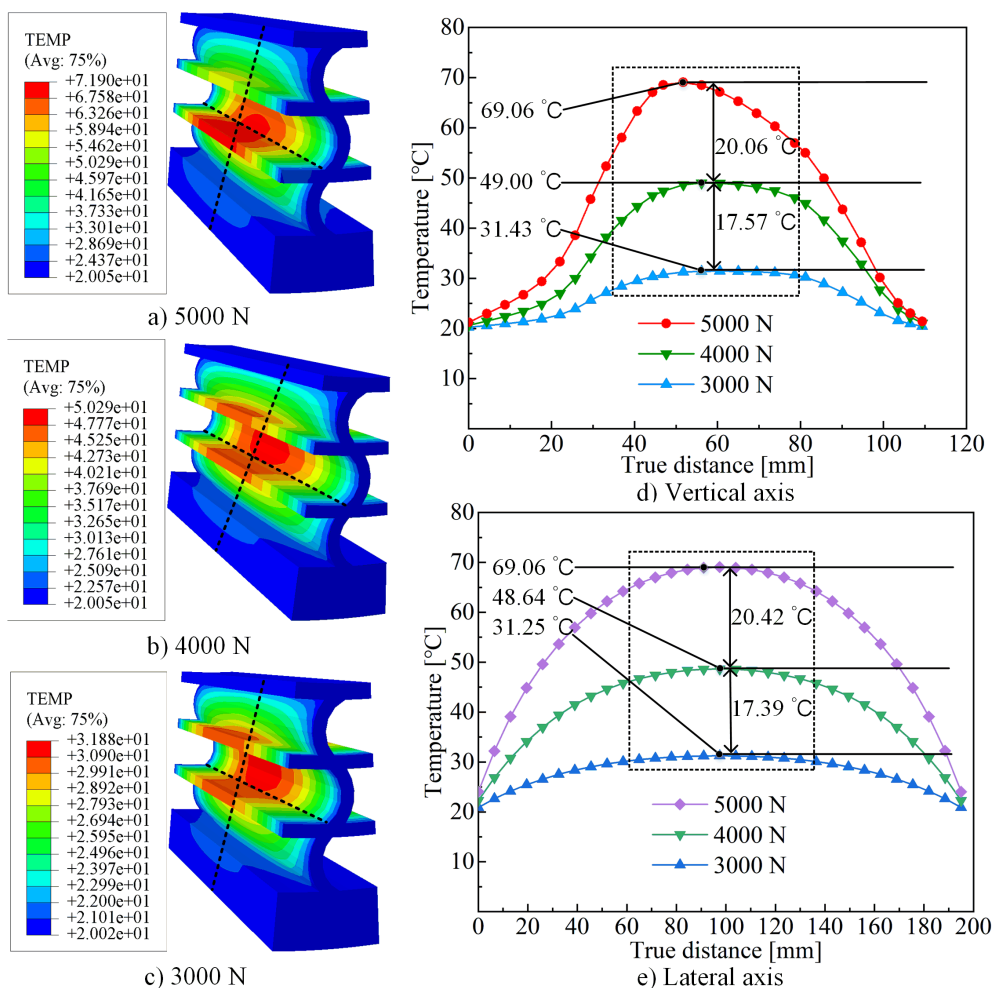
Fig. 10. *Steady-state temperature field distribution under different loads*

indicates that the influence of the load change on the temperature of the flexible spoke non-pneumatic tire has nothing to do with the loading conditions of the tire.

4 CONCLUSIONS

The 3D model and numerical analysis model of the 195/50N16 flexible spoke non-pneumatic tire were established based on the unit configuration method. The thermo-mechanical sequential coupling method was used to carry out a deformation analysis, an energy loss analysis, and a heat conduction analysis on the flexible-spoke non-pneumatic tire. The temperature distribution of the flexible spoke non-pneumatic tire under the influence of thermo-mechanical coupling was obtained. After comparative analysis, the conclusions are as follows:

1. The high temperature region of the flexible spoke non-pneumatic tire is mainly concentrated in the middle bending part of the flexible spoke unit, which is consistent with the main stress deformation part. The overall temperature gradually decreases from the centre of the flexible spoke to the surrounding parts.

2. Under the condition of constant vertical load, the overall temperature and the maximum temperature of the non-pneumatic tire increase slightly with the increase of the driving speed. The centre temperature of the flexible spoke unit is higher than the edge temperature of the flexible spoke unit, and with the increase of the driving speed, the temperature rise of the centre of the flexible spoke unit is greater than that of the edge of the flexible spoke unit. The influence of the driving speed on the temperature change of

the non-pneumatic tire is greater at higher speeds than that at lower speeds.

3. Under the condition of constant driving speed, the overall temperature and the maximum temperature of the non-pneumatic tire increase significantly with the increase of the load. The centre temperature of the flexible spoke unit is higher than the edge temperature of the flexible spoke unit. With the increase of the vertical load, the temperature rise of the centre of the flexible spoke unit is significantly greater than that of the edge of the flexible spoke unit, and the overall temperature rise is larger. The influence of load change on the temperature of the flexible spoke non-pneumatic tire has nothing to do the loading conditions of the tire.

4. Both the driving speed and the vertical load affect the overall temperature and the maximum temperature of the flexible spoke non-pneumatic tire. However, the load has a significantly larger influence on the temperature change than the driving speed. Therefore, it is possible to increase the driving speed appropriately under the condition of reducing the load, and thus solve the problem of high temperature failure caused by high-speed operation for current non-pneumatic tires.

5 ACKNOWLEDGEMENTS

6 REFERENCES

[1] Zhang, Z.F., Fu, H.X., Liang, X. M., Chen, X. X., Tan, D. (2020). Comparative analysis of static and dynamic performance of non-pneumatic tire with flexible spoke structure. *Strojniški vestnik - Journal of Mechanical Engineering*, vol. 66, no. 7-8, p. 458-466, **DOI:10.5545/sv-jme.2020.6676**.

[2] Zhang, Z.Z., Lv, J.G., Song, B., Guo, S.Y., Gao, F. (2013). Development of Non-Pneumatic Tire Technology. *Applied Mechanics and Materials*, vol. 427-429, p. 191-194, **DOI:10.4028/www.scientific.net/AMM.427-429.191**.

[3] Mathew, N.J., Sahoo, D.K., Chakravarthy, E.M. (2017). Design and static analysis of airlesstyre to reduce deformation. *Materials Science and Engineering Conference Series*, vol. 197, **DOI:10.1088/1757-899X/197/1/012042**.

[4] Veeramurthy, M. (2011). *Modeling, Finite Element Analysis, and Optimization of Non-Pneumatic Tire (NPT) for the Minimization of Rolling Resistance*. BSc Thesis, Clemson University, Clemson.

[5] Narasimhan, A., Ziegert, J., Thompson, J. (2011). Effects of material properties on static load-deflection and vibration of a non-pneumatic tire during high-speed rolling. *SAE International Journal of Passenger Cars-Mechanical Systems*, vol. 4, no. 1, p. 59-72, **DOI:10.4271/2011-01-0101**.

[6] Ju, J., Kim, D.-K., Kim, K. (2012). Flexible cellular solid spokes of a non-pneumatic tire. *Composite Structures*, vol. 94, no. 8, p. 2285-2295, **DOI:10.1016/j.compstruct.2011.12.022**.

[7] Zhao, Y.Q., Zhu, M.M., Lin, F., Xiao, Z., Li, H.Q., Deng, Y.J. (2018). Thermal modal analysis of novel non-pneumatic mechanical elastic wheel based on FEM and EMA. *AIP Advances*, vol. 8, art. ID 015229, **DOI:10.1063/1.5018488**.

[8] Wang, Z.P. (2010). Finite element analysis of mechanical and temperature field for a rolling tire. *International Conference on Measuring Technology and Mechatronics Automation*, p. 278-283, **DOI:10.1109/icmtma.2010.42**.

[9] Gasmi, A., Joseph, P.F., Rhyne, T.B., Cron, S.M. (2012). Development of a two-dimensional model of a compliant non-pneumatic tire. *International Journal of Solids & Structures*, vol. 49, no. 13, p. 1723-1740, **DOI:10.1016/j.ijsolstr.2012.03.007**.

[10] Kucewicz, M., Baranowski, P., Maachowski, J. (2016). Airless tire conceptions modeling and simulations. *1st Renewable Energy Sources-Research and Business*, p. 293-301, **DOI:10.1007/978-3-319-50938-9_30**.

[11] Xu, H., Zhao, Y.Q., Ye, C., Lin, F. (2019). Integrated optimization for mechanical elastic wheel and suspension based on an improved artificial fish swarm algorithm. *Advances in Engineering Software*, vol. 137, art. ID 102722, **DOI:10.1016/j.advengsoft.2019.102722**.

[12] Mazur, V.V. (2020). Experiments to find the rolling resistance of non-pneumatic tires car wheels. *Proceedings of the 5th International Conference on Industrial Engineering*, p. 641-648, **DOI:10.1007/978-3-030-22041-9_69**.

[13] Ju, J., Veeramurthy, M., Summers, J.D., Thompson, L.L. (2013). Rolling resistance of a non-pneumatic tire having a porous elastomer composite shear band. *Tire Science & Technology*, vol. 41, no. 3, p. 154-173, **DOI:10.2346/tire.13.410303**.

[14] Jackowski, J., Wieczorek, M., Żmuda, M. (2018). Energy consumption estimation of non-pneumatic tire and pneumatic tire during rolling. *Journal of KONES Powertrain and Transport*, vol. 25, no. 1, p. 159-168, **DOI:10.5604/01.3001.0012.2463**.

[15] Fu, H.X., Zhao, Y.Q., Du, X.B., Wang, Q., Xiao, Z. (2017). Analysis on influencing factors of lateral stiffness of mechanical elastic wheel. *Journal of Shanghai Jiaotong University*, vol. 51, no. 7, p. 863-869, **DOI:10.16183/j.cnki.jsjtu.2017.07.014.** (in Chinese)

[16] Fu, H.X., Zhao, Y.Q., Lin, F., Du, X.B., Zhu, M.M. (2017). Steady-state cornering properties of a non-pneumatic tire with mechanical elastic structure. *Transactions of Nanjing University of Aeronautics and Astronautics*, vol. 34, no. 5, p. 586-592, **DOI:10.16356/j.1005-1120.2017.05.586.** (in Chinese)

[17] Zang, L.G., Zhao, Y.Q., Li, B., Wang, J., Fu, H.X. (2016). An experimental study on the ground contact characteristics of non-pneumatic mechanical elastic wheel. *Automotive*

Engineering, vol. 38, no. 3, p. 350-355, **DOI:10.19562/j. chinasae.qcgc.2016.03.014.** (in Chinese)

[18] Du, X.B., Zhao, Y.Q., Wang, Q., Fu, H.X., Lin, F. (2019). Grounding characteristics of a non-pneumatic mechanical elastic tire in a rolling state with a camber angle. *Strojniški vestnik-Journal of Mechanical Engineering*, vol. 65, no. 5, p. 287-296, **DOI:10.5545/ sv-jme.2018.5845**.

[19] Sriwijaya, R., Hamzah, R. (2019). The effect of surface contact on the pressure distribution and deflection of airless tires. *AIP Conference Proceedings*, vol. 2187, art ID. 050021, **DOI:10.1063/1.5138351**.

[20] Zhang, T.H., Xu, Z., Wang, W. (2018). Finite element analysis and prediction on static grounding performance and fatigue life of staggered non-pneumatic tire. *China Rubber Industry*, vol. 65, no. 12, p. 1383-1386. (in Chinese)

[21] Li, Q.L., Fan, L.C., Li, T. (2011). Determination of thermo-physical properties of rubber and its effect on curing temperature field of tire. *Advanced Materials Research*, vol. 221, p. 533-539, **DOI:10.4028/www.scientific.net/ AMR.221.533.**

[22] Yan, X.Q. (2007). A numerical modeling of dynamic curing process of tire by finite element. *Polymer Journal*, vol. 39, p. 1001-1010, **DOI:10.1295/polymj.pj2006182**.

[23] Chen, Y.Q., Zhao, Y.Q., Ruan, M.Q., Li, B., Zang, L.G. (2016). Finite element analysis on steady-state temperature field of a rolling mechanical elastic wheel. *Mechanical Science & Technology for Aerospace Engineering*, vol. 35, no. 3, p. 364-369, **DOI:10.13433/j.cnki.1003-8728.2016.0307.** (in Chinese)

[24] Zhu, M.M., Zhao, Y.Q., Xiao, Z., Deng, Y.J. (2018). Surface temperature prediction of novel non-pneumatic mechanical elastic wheel based on theory analysis and experimental verification. *Numerical Heat Transfer Part B: Fundamentals*, vol. 73, no. 6, p. 399-414, **DOI:10.1080/10407790.2018.149 1721.**